Carcinogenesis, 2022, **43**, 1059–1070
https://doi.org/10.1093/carcin/bgac075
Advance access publication 7 September 2022
Original Article

Original Article

LAMTOR1 degrades MHC-II via the endocytic in hepatocellular carcinoma

Bo Wu[1], Qian Wang[2], Bowen Li[3] and Meixi Jiang[4,*]

[1]Department of General Surgery, The Fourth Affiliated Hospital, China Medical University, Shenyang 110032, China,
[2]Department of Radiology, The Fifth Hospital of Xiamen, Xiamen 361101, China,
[3]Department of Oncological and Endoscopic Surgery, The First Affiliated Hospital of Harbin Medical University, Harbin 150000, China and
[4]Department of Neurology, The Fourth Affiliated Hospital, China Medical University, Shenyang 110032, China

*To whom correspondence should be addressed. Tel: +86 13782206769; Fax: +86 02462255001; Email: jmx13782206769@163.com

Abstract

Tumor cell surface antigen recognition is a major hallmark of cancer therapy, and loss of major histocompatibility complex class I (MHC-I) is the most common mechanism that impairs tumor cell surface antigen processing and expression. In addition to this, MHC-II regulates antigen presentation in $CD4^+$ T cell immune responses involved in tumor killing by $CD8^+$ T cells, whereas the regulation of endocytosis regulating MHC-II antigen presentation has not been reported. Therefore, the regulation of the endocytosis pathway on the expression of MHC-II surface level and antitumor T cell response remains to be explored. In this experiment, we found that LAMTOR1 regulates the endocytic pathway through the GTPase domain of DNM2 and triggers the formation of autophagosomes. We performed flow cytometry and western blotting analyses, which revealed that the expression of MHC-II molecules on the surface of cells is influenced by LAMTOR1 through the endocytic pathway. We showed that the expression of MHC-II molecules, which recognize $CD4^+$ T cells on the surface of cells, was regulated by LAMTOR1 through an endocytic pathway. By coculture experiments, we showed that $CD8^+/CD4^+$ T cells exhibit substantially higher levels of tumor cell apoptosis than those observed when hepatocellular carcinoma (HCC) cells were cocultured with $CD8^+$ T cells alone. This study revealed that LAMTOR1 decreases the expression levels of MHC-II on cell surfaces in order to reduce antigen expression, leading to a decrease in antitumor T cell responses.

Graphical Abstract

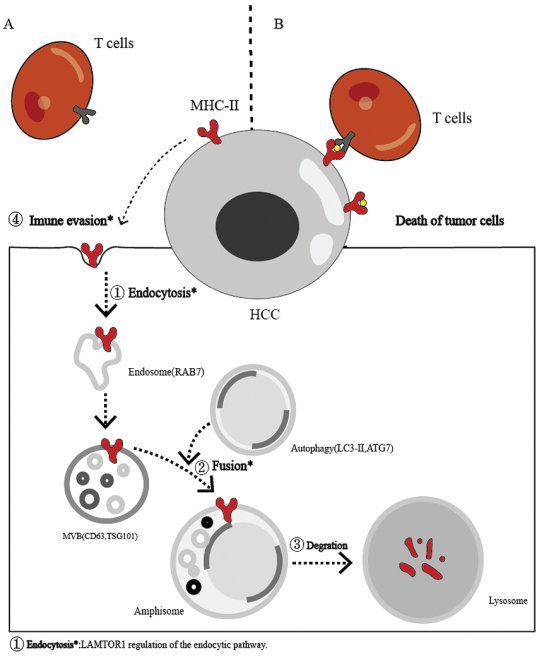

Received: April 17, 2022; Revised: August 11 2022; Accepted: September 6, 2022

LAMTOR1 promotes immune escape by targeting MHC-II molecules via endocytic degradation in HCC (graphical_abstract). Therefore, LAMTOR1 may be used clinically as a specific biomarker for screening HCC or as a potential target for individualized patient therapies.

Abbreviations: AAV8, Adeno-associated virus serotype 8; Ag, antigens; APCs, antigen-presenting cells; Co-IP, co-immunoprecipitation; CTL, cytotoxic T lymphocytes; EDU, 5-Ethynyl-2′-deoxyuridine; GO, Gene Ontology; HCC, hepatocellular carcinoma; ICT, immune checkpoint blockade therapy; IHC, immunohistochemistry; KEGG, Kyoto Encyclopedia of Genes and Genomes; LAMTOR1, late endosomal/lysosomal Adaptor, MAPK and mTOR activator 1; MHC-I, major histocompatibility complex class I; MHC-II, major histocompatibility complex class II; OS, Overall survival; TCGA, The Cancer Genome Atlas; TCR, T cell receptors; TME, tumor microenvironment

Introduction

Hepatocellular carcinoma (HCC) is one of the most common cancer types in the world (1). Major histocompatibility complex class I (MHC-I) is an important target for tumor-specific $CD8^+$ cytotoxic T lymphocytes. Loss of major histocompatibility complex class I (MHC-I) is the most common mechanism of immune escape of tumor cells. In addition to this, MHC-II regulates antigen presentation in $CD4^+$ T cell immune responses and is involved in tumor killing by $CD8^+$ T cells. However, the effect of MHC-II on $CD4^+$ T cell immune responses affecting tumor presentation of antigens has not been recognized until recently (2–5).

Cells exhibit endocytic responses to immune evasion by delivering MHC-II to lysosomes for degradation (6,7). Endocytosis and autophagy can occur synergistically to promote their optimal behavior (8, 9). Both processes may be involved in lysosomal degradation through the formation of amphisomes (10). Endocytosis begins with the internalization of plasma membrane cargo into endosomes, labeled by specific ligand proteins and small Rab GTPases (11,12). Various autophagic molecules can be localized to recycling endosomes (13–16). In addition, studies have established that the function of endosome-associated genes is associated with the regulation of autophagic vesicle maturation, closure and merging with lysosomes (17–19). It is also reported that the formation of endosomes and autophagosomes, which induces the production of amphisome bodies (20). Several studies have implicated the role of LAMTOR1 in cellular metabolism, which induced autophagy formation and the anchoring of the MEK-ERK pathway to late endosomes (21,22). Therefore, we aimed to study that LAMTOR1 promotes immune escape by targeting MHC-II molecules via endocytic degradation in HCC.

Materials and methods

Cell culture

The cell lines L02, Huh7, HepG2 and mouse Hepa1-6 were procured from the American Type Culture Collection (ATCC, Manassas, VA). The cell lines L02, Huh7, HepG2 and mouse Hepa1-6 were cultured by DMEM (Gibco, Grand Island, USA) supplemented with 10% fetal bovine serum and penicillin (10 000 U/mL), streptomycin (0.1 mg/mL) medium and grown in a constant temperature humidified incubator at 37°C and 5% CO2. All cell experiments were validated using Huh7, HepG2 and Hepa1-6 cell lines, while Hepa1-6 cell lines were used in the animal experiments. The cells were cytogenetically tested and authenticated using the short tandem repeat method. All cell-based experiments were carried out on cells that have been tested for <12 weeks. The cell lines were lasted tested in March 2022.

Antibodies and reagents

The antibodies used were: anti-LAMTOR1 (catalog #8943S;CST), anti-dynamin 2 (DNM2; catalog #ab3457; Abcam), anti-RAB5 (catalog #E6N8S;CST), anti-TSG101 (catalog #GTX70255;GeneTex), anti-RAB35 (catalog #GTX120249;GeneTex), anti-RAB7 (catalog #E9O7A;CST), anti-VPS26A (catalog #ab181352;Abcam), anti-P62 (catalog #D5L7G;CST), anti-LC3B (catalog #E5Q2K;CST), anti-HLA-A (catalog #ab52922;Abcam), anti-HLA-B (catalog #ab193415;Abcam), anti-HLA-C (catalog #ab126722;Abcam) and anti-MHC-II (catalog #ab55152;Abcam).

The reagents used were: 1 μM Dynasore (catalog #HY-15304;MedChemExpress), 5 mM 3-methyl adenine (3-MA;autophagy inhibitor) (catalog #HY-19312; MedChemExpress) and 10 nM mammalian target of rapamycin (RAP;HY-10219; MedChemExpress).

Mouse experiments

Mice were anesthetized and 1×10^6 Hepa1-6 cells were suspended in Hank's balanced salt solution and injected into the left lobe of the mouse liver with an insulin syringe. Then, the peritoneum was sutured and the skin was closed. Mice were euthanized after 2–3 weeks and samples were collected after transcardial perfusion with phosphate-buffered saline (PBS).

Cell transfection

Cell lines with LAMTOR1 overexpression (*LAMTOR1*-OE) and short hairpin RNA (shRNA; sh-*LAMTOR1*) knockdown were generated by lentiviral systemic culture; lentiviral transfection was also performed, targeting the shRNA of *RAB7A* and *ATG7*. To generate stably expressed cell lines, puromycin screening (2 μg/mL) was performed after cell transfection:

sh-*LAMTOR1*-1: 5′-CCCATCCCGTTCTCTGATTTG-3′
sh-*LAMTOR1*-2: 5′-CATGGAGCAGCATGAGTACAT-3′
RAB7A: 5′-AGGCTAGTCACAATGCA-GATA-3′
ATG7: 5′-CTGCTGAGGAGCTCTCCAT-3′

Immunoblotting

Total proteins were separated by SDS-PAGE electrophoresis, transferred to polyvinylidene difluoride (PVDF) membranes, blocked bovine serum albumin (BSA), incubated with antibody.

Immunofluorescence assay

Cells were cultured on coverslips for 1–2 days. After apposition, cells were washed, fixed, blocked and incubated with antibody and nuclei were stained using DAPI, placed on slides and Nikon A1R confocal microscope with 60× and 20× objectives were observed.

Histology and immunohistochemistry

Human hepatocellular carcinoma specimens (HCC) tumor samples (n = 45) were collected from the patients who received surgery at China Medical University and Xuchang Central Hospital, Henan University of Science

and Technology from November 2019 to January 2020. All patients had histologically confirmed HCC. Patients with neoadjuvant treatment, inflammatory diseases, or active infection were excluded. Informed consent was obtained before sample collection. The study was approved by the Committee for the Ethical Review of Research, China Medical University.

All protocols utilized for hepatocellular carcinoma specimens were approved by Chinese Medical University. Hepatocellular carcinoma tissues were stained by using LAMTOR1 (1:500;CST,3868) and CD4 (1:400;ab133616;Abcam) and determine protein expression.

RNA sequencing analysis

Total RNA was extracted from HCC cells and sequenced on an Illumina HiSeq 2500 System (San Diego, CA, USA). Enrichment analysis of sh-*LAMTOR1* with sh-Ctrl in Huh7 cells was performed using the Metascape platform (fold-change > 1.0, adjusted *P*-value < 0.05).

TCGA dataset analysis

We retrieved 371 HCC samples with detailed gene expression data and clinical features from The Cancer Genome Atlas (TCGA) database and analysed the relationship between *LAMTOR1* and related functions from these samples.

Co-immunoprecipitation

Co-immunoprecipitation (co-IP) kits (catalog #ab206996, Abcam) were used to study the relationship between LAMTOR1 and DNM2. LAMTOR1 protein (2 μg) was incubated with DNM2 (5 μg) or its deletion constructs 1/2/3 in an *in vitro* co-IP assay. LAMTOR1 was then detected with antibody LAMTOR1 (D1H6) and the deletion structure of the protein was detected with a 6xHis antibody.

Tumor and T cell coculture experiments and detection of apoptotic tumor cells

$CD3^+$ T cells were harvested from splenocytes of mice by flow cytometry and sorted for $CD4^+$ T as well as $CD8^+$ T cells. Hepa1-6 cells and $CD8^+$ T and $CD4^+$ T cells were cultured with 50% Dulbecco's modified Eagle's medium (DMEM) and 50% RPMI-1640,10% FBS. Hepa1-6 cells were detected in the apoptosis rate by flow cytometry.

Adeno-associated virus serotype 8 (AAV8) production

Three plasmids were transfected with HEK293T cells to prepare the virus, including rAAV-shRNA-EGFP, an AAV helper plasmid (containing Rep and Cap genes) and an adenovirus helper plasmid (pAD). All recombinant AAV vectors were derived from AAV8. AAV8 vectors use the H1 promoter to express *LAMTOR1* siRNA or interfering control siRNA, while the cytomegalovirus virus promoter drives EGFP reporter expression.

Statistical analyses

All experimental results were repeated at least 3 times and statistical significance was calculated using ANOVA. For ANOVA, nonparametric tests were performed by comparing the median of all groups with $P < 0.05$.

Results

Association of LAMTOR1 with the clinical pathology in hepatocellular carcinoma

To screen key vesicle trafficking factors regulating HCC, we analysed the function of five gene sets using KEGG datasets, in which LAMTOR1 was identified as a signature factor (Figure 1A). Several studies have implicated the role of LAMTOR1 in cellular metabolism, including the anchoring of the MEK-ERK pathway to late endosomes via LAMTOR1 (21,22). Although its mechanism has not been elucidated, LAMTOR1 is highly expressed in HCC according to the TCGA dataset ($P<0.01$) (Figure 1B). To determine the clinical significance of LAMTOR1, we found that the positive relationship between LAMTOR1 and stage ($P = 0.001$) as well as prognostic ($P = 0.002$) (Figure 1C–E). Fluorescence microscopy images showed endogenous LAMTOR1 protein distribution in human HCC tissues (Figure 1F). The expression of LAMTOR1 was increased in Huh7, HepG2 and Hepa1-6 cell lines compared with L02 cell lines ($P < 0.05$) (Figure 1G). Moreover, the expression of LAMTOR1 was higher in HCC tissues compared with adjacent tissues ($n = 45$) ($P < 0.05$) (Figure 1H). We performed a univariate analysis using information from pan-cancer entries in TCGA datasets and found that high expression of LAMTOR1 was a risk factor for overall survival (OS) ($P < 0.05$) and disease-free survival (DSS) in HCC ($P < 0.05$) (Figure 1I and J). The levels of LAMTOR1 were evaluated in HCC tissues ($n = 45$) and compared with patients' OS ($P = 0.011$) (Supplementary Figure S1K and L available at *Carcinogenesis* Online). We also found that LAMTOR1 expression was significantly related to the stage ($P = 0.0006$) (Table 1). These findings revealed that LAMTOR1 is an oncogenic gene in HCC.

Regulation of the endocytic pathway by LAMTOR1 is dependent on DNM2

LAMTOR1 controls cell growth by regulating the balance of energy metabolism (23). The potential pathways imply that high LAMTOR1 expression related with endocytic pathways (Figure 2A). We also analysed LAMTOR1 dependent transcriptome in parental and *LAMTOR1* knockout (KO) Huh7 cells through RNA sequencing (RNA-Seq) (Figure 2B). Given that endosomes are one of the hallmarks of endocytic pathways, the expression of several markers was tested as shown in the results. HCC tissues showed a punctate cytoplasmic distribution of LAMTOR1 colocalized with early endosomes (RAB5) and late endosomes (RAB7) (Supplementary Figure S2A and C available at *Carcinogenesis* Online). Moreover, *LAMTOR1* knockdown resulted in a decreased number of late endosomes (Figure 2D) and decreased perinuclear internalization of EGFR ($P < 0.05$) (Supplementary Figure S2B and C available at *Carcinogenesis* Online).

The endocytic pathway refers to the regulation of substance internalization through the formation of 60–120 nm vesicles by invagination of the cytoplasmic membrane, which wraps external substances and imports them into the cell (24–27). We investigated the mechanisms underlying LAMTOR1-induced endocytosis signaling in HCC and identified 17 genes that were substantially differentially expressed. We clustered these hub genes and found that *DNM2*, *RAB5*, *RAB7*, *RAB35*, *VPS26A* and *TSG101* were influenced by LAMTOR1 in the

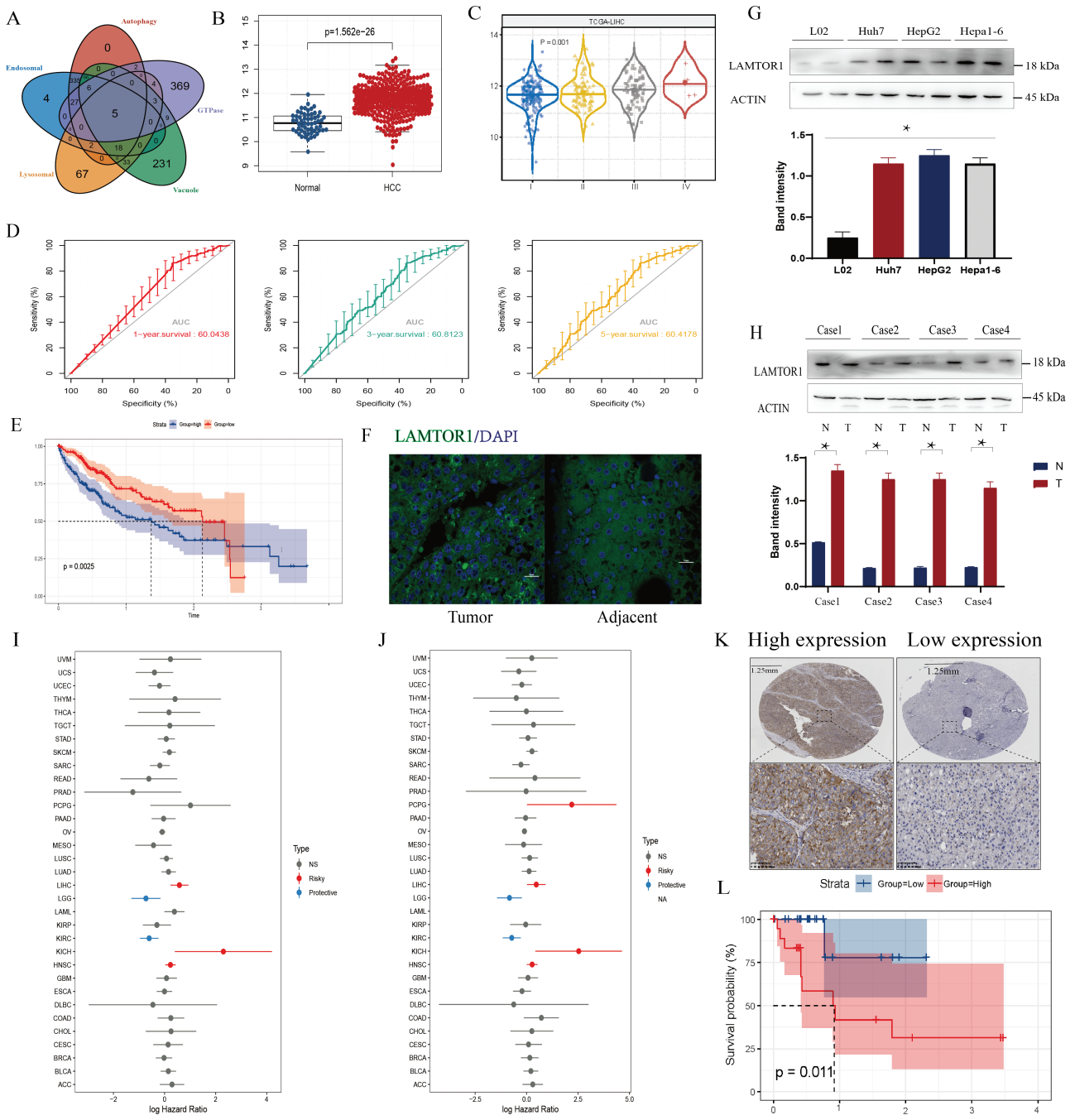

Figure 1. Upregulated expression of LAMTOR1 in relation with oncogenes in hepatocellular carcinoma (HCC). (**A**) Venn diagram showing the function of five gene sets in vesicle trafficking based on Kyoto Encyclopedia of Genes and Genomes (KEGG) dataset. (**B**) LAMTOR1 protein levels analysed by The Cancer Genome Atlas (TCGA) database in HCC and adjacent tissues. (**C–E**) Correlation of LAMTOR1 with clinical characteristics, area under the curve evaluation (AUC) and prognostic value of overall survival (OS) in patients with HCC based on the TCGA dataset. (**F**) Fluorescence microscopy images showing the LAMTOR1 protein distribution in human HCC and adjacent tissues. Scale bar: 20 μm. (**G**) LAMTOR1 protein expression in HCC cell lines compared with normal liver cell lines. (**H**) LAMTOR1 protein expression in HCC and adjacent tissues. (**I, J**) Overall survival (OS) and disease-free survival (DFS) of patients with pan-cancer according to the TCGA datasets. (**K, L**) Representative graphs of immunohistochemical (IHC) staining for LAMTOR1 expression in 45 HCC patients (scale bar: 1.25 mm; scale bar: 200 μm).

TCGA database (Figure 2E). We verified these results in parental and *LAMTOR1* KO Huh7 cells by RNA sequencing (RNA-Seq) (Figure 2F). Immunoblotting was also performed to demonstrate that *LAMTOR1* knockdown decreased RAB7, RAB35 and TSG101 ($P < 0.05$) (Figure 2G). Time-lapse microscopy indicated that sh-*LAMTOR1* decreased endocytic speed (Figure 2H), confirming that LAMTOR1 induces the endocytic process.

DNM2 GTPase is a key step in the regulation of the separation of endosomal vesicles from the plasma membrane (28). We found that prolonged Dynasore inhibition leads to increased expression of early endosomes (RAB5) and late endosomes (RAB7) ($P < 0.05$) (Supplementary Figure S2D available at *Carcinogenesis* Online). To further explore the association of LAMTOR1–DNM2 interaction, co-immunoprecipitation was performed on a panel of HCC

Table 1. Association between the expression of LAMTOR1 and clinicopathological features of HCC patients

Characteristics	No.	High LAMTOR1	Low LAMTOR1	*P*-value
		(Q Score ≥ 150; *n* = 20)	(Q Score < 150; *n* = 25)	
Age(y)				0.4227
<60	21	8	13	
≥60	24	12	12	
Sex				0.5403
Female	18	7	11	
Male	27	13	14	
Tumor size (cm)				0.0662
<5.0	18	5	13	
≥5.0	27	15	12	
Tumor differentiation				0.2426
Well	2	1	1	
Moderate	18	8	10	
Poor	25	11	14	
Stage				0.0006*
I–II	23	4	19	
III–IV	22	16	6	
Vessel infiltration				0.6067
Negative	32	15	17	
Positive	13	5	8	

All statistical tests are two-sided.

cell lines (Figure 2I). For a more detailed mapping of the D-terminal region of DNM2, three domains were expressed: construct 1: full-length domain, construct 2: partial deletion in GTPase domain and construct 3: full GTPase domain deleted (Figure 2J). The binding of these constructs to LAMTOR1 was assessed using *in vitro* immunoprecipitation, and deletion of part of the GTPase domain (23 amino acids) or full GTPase domain abrogated binding to LAMTOR1 (Figure 2K). These results suggest that LAMTOR1 regulates endocytosis by interacting with the GTPase domain of DNM2.

LAMTOR1 induces the endocytic pathway to form amphisomes

Enrichment of intracellular autophagy and lysosomes can be observed following increased activity of LAMTOR1 (29). We found that LC3-I expression levels increased ($P < 0.05$) and P62 expression levels remarkably decreased ($P < 0.05$) in the sh-*LAMTOR1* group (Supplementary Figure S3A available at *Carcinogenesis* Online). Furthermore, transmission electron microscopy revealed a decrease in the number of autophagosomes after treatment with sh-*LAMTOR1* (Supplementary Figure S3B available at *Carcinogenesis* Online). In response to stress, cells initiate endocytosis and autophagy to maintain cellular homeostasis (30,31). This leads to the formation of amphisomes, which are hybrid organelles that play a key role in the cross-talk between endosomes and autophagy (32). We investigated whether LAMTOR1 induced the fusion of endosomes and autophagosomes. It was revealed that CD63, and TSG101 were strongly colocalized with LC3B in sh-Ctrl but not sh-*LAMTOR1* ($P < 0.05$) (Supplementary Figure S3C and E available at *Carcinogenesis* Online). Confocal images showed higher LC3B colocalization with CD63 and TSG101 in HCC tissues (Supplementary Figure S3D and F available at *Carcinogenesis* Online). We also found that LC3 and CD63 were strongly colocalized with LAMP1 in sh-Ctrl but not in sh-*LAMTOR1* cells ($P < 0.05$) (Supplementary Figure S3G and H available at *Carcinogenesis* Online). LAMP1 colocalization with LC3 and LAMP1 in HCC tissues than adjacent tissues (Supplementary Figure S4A available at *Carcinogenesis* Online). Confocal images showed higher CD63 colocalization with LAMP1 in HCC tissues (Supplementary Figure S4B available at *Carcinogenesis* Online). These results suggest that activation of LAMTOR1 triggers the formation of endosomes and autophagosomes, which induces the production of amphisome bodies.

LAMTOR1 regulates cell adhesion molecules by endocytosis

Endocytosis contributes to the characterization of the migratory behavior of tumor cells (33–36). We used the TCGA database to analyse the correlation between endocytosis and cell adhesion molecules, immunity, cell stemness and extracellular vesicles. We extracted the molecules related to endocytosis in the KEGG database using R, and analysed the correlation with cell adhesion molecules (Supplementary Figure S5A–D available at *Carcinogenesis* Online). To analyse the correlation of endocytosis with other signaling pathways, we showed that endocytosis was remarkably associated with cell adhesion molecules, suggesting a potential role of endocytosis in the regulation of tumor cell proliferation and migration (Supplementary Figure S6A and B available at *Carcinogenesis* Online). The Gene Set Enrichment Analysis showed that LAMTOR1 expression was correlated with cell adhesion molecules (Supplementary Figure S6C available at *Carcinogenesis* Online). We further examined the potential role of LAMTOR1 in cell adhesion molecule gene sets

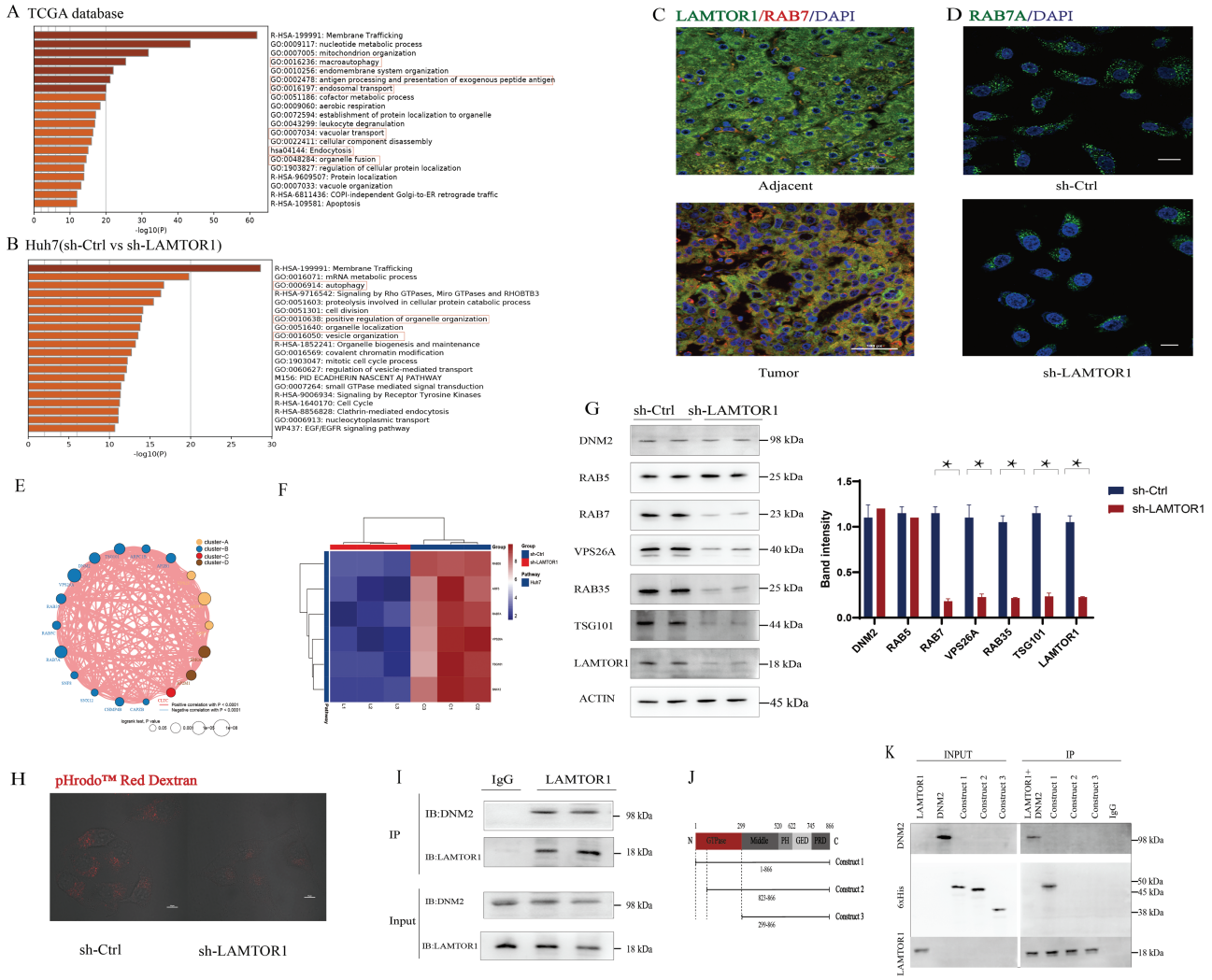

Figure 2. Regulation of endocytosis by LAMTOR1 is DNM2-dependent. (**A**) KEGG/Gene Ontology (GO) analysis shows signaling pathways that were substantially affected by LAMTOR1 in the TCGA database. (**B**) KEGG/GO analysis shows the signaling pathways affected by LAMTOR1 in RNA sequences. (**C**) Confocal microscopy of endogenous LAMTOR1 and RAB7 (red) in HCC and adjacent tissues. Scale bar: 20 μm. (**D**) Immunofluorescence detection of RAB7 of control (short hairpin [sh]-control [Ctrl]) and LAMTOR1 knockdown (sh-*LAMTOR1*) groups as observed by confocal microscopy. Scale bar: 20 μm. (**E**) Correlation of *LAMTOR1*-related genes was analysed based on TCGA datasets. (**F**) Expression of *LAMTOR1* based on RNA sequences using heat map showing the expression of six genes in HCC. (**G**) Huh7, HepG2 and Hepa1-6 cells were transfected with sh-Ctrl and sh-*LAMTOR1* and western blot was performed, which showed endocytosis hub gene expression. (**H**) sh-Ctrl and sh-*LAMTOR1* groups were incubated with pH rodo™ Red dye for time-lapse real-time imaging. (**I**) Detection by co-immunoprecipitation between LAMTOR1 and DNM2 interaction. (**J**) Interaction between LAMTOR1 and DNM2 was constructed by detailed mapping of DNM2. (**K**) D-terminal GTPase region of DNM2 interacting with LAMTOR1 was assessed using *in vitro* immunoprecipitation assay.

using Gene Ontology (GO) analysis. The results showed that LAMTOR1 associated with MHC class II protein complex, T cell costimulation and antigen processing and presentation (Supplementary Figure S6D available at *Carcinogenesis* Online). This suggests that LAMTOR1 has positive effects on cell adhesion molecules of antigen processing. LAMTOR1 was found to be associated with cell adhesion molecules (Supplementary Figure S5E available at *Carcinogenesis* Online) and revealed CD4 based on GSE140228 datasets (Supplementary Figure S5F available at *Carcinogenesis* Online). We also evaluated the role of LAMTOR1 on the migration and proliferation of HCC cell lines using Transwell and 5-ethynyl-2′-deoxyuridine (EdU) assays. Notably, treatment with sh-*LAMTOR1* decreased tumor growth ($P < 0.05$) (Supplementary Figure S6E and F available at *Carcinogenesis* Online). Confocal imaging showed higher MHC-II (red) colocalization with CD63 (green) in HCC tissues compared with adjacent tissues (Supplementary Figure S6G available at *Carcinogenesis* Online). Confocal imaging further showed higher MHC-II (green) colocalization with LC3B (green) in HCC tissues compared with adjacent tissues (Supplementary Figure S6H available at *Carcinogenesis* Online). These results showed that activation of LAMTOR1 regulated MHC-II molecules through endosome and autophagosome formation.

LAMTOR1 degrades plasma surface MHC-II by endocytosis

We found that LAMTOR1 inversely regulates the expression of MHC-II ($P<0.05$) (Supplementary Figure S7A and B available at *Carcinogenesis* Online). MHC-I is regulated by autophagy, while MHC-II is regulated by autophagy as well as endocytosis, demonstrating that MHC-II degradation

pathway different with MHC-I ($P < 0.05$) (Supplementary Figure S7C and D available at *Carcinogenesis* Online). To gain insights into LAMTOR1 is involved in MHC-II degradation, We constructed LAMTOR1, RAB7 and ATG7 stable transduction cell lines to clarify the whole cell expression of MHC-II regulation by LAMTOR1 through RAB7 (endosomal) and ATG7 (autophagy). We found that the degradation of MHC-II molecules by LAMTOR1 through endocytosis and autophagy (Figure 3A). To explore LAMTOR1 exchange plasma membrane MHC-II levels in HCC cells, we separated MHC-II molecules on the cell membrane surface by sucrose density gradient centrifugation and detected them by western blotting ($P < 0.05$) (Figure 3B). Next, to test the expression of MHC-II molecules on the plasma membrane, we performed flow cytometric analysis to demonstrate that LAMTOR1 regulates changes in the levels of MHC-II molecules on the cell membrane surface through endocytic pathways (Figure 3C and D). Immunofluorescence staining showed drastically attenuated colocalization of LAMTOR1 with MHC-II after the knockdown of *RAB7* and *ATG7* (Figure 3E and F). The results show that LAMTOR1 degrades cell surface MHC-II through endocytosis.

LAMTOR1 degrades cell surface MHC-II to promote immune escape

Next, multiplex immunofluorescent staining and multispectral imaging were used to identify LAMTOR1, RAB7 and MHC-II coexpression in HCC cells (Figure 4A). We hypothesized that endocytic pathway-induced reduction in the surface levels of MHC-II might contribute to their immune escape from CD4⁺ T cell recognition. Therefore, we found that the expression of LAMTOR1 negative associated with CD4⁺ T cell infiltration in HCC patients from China Medical University by immunohistochemical (IHC) staining

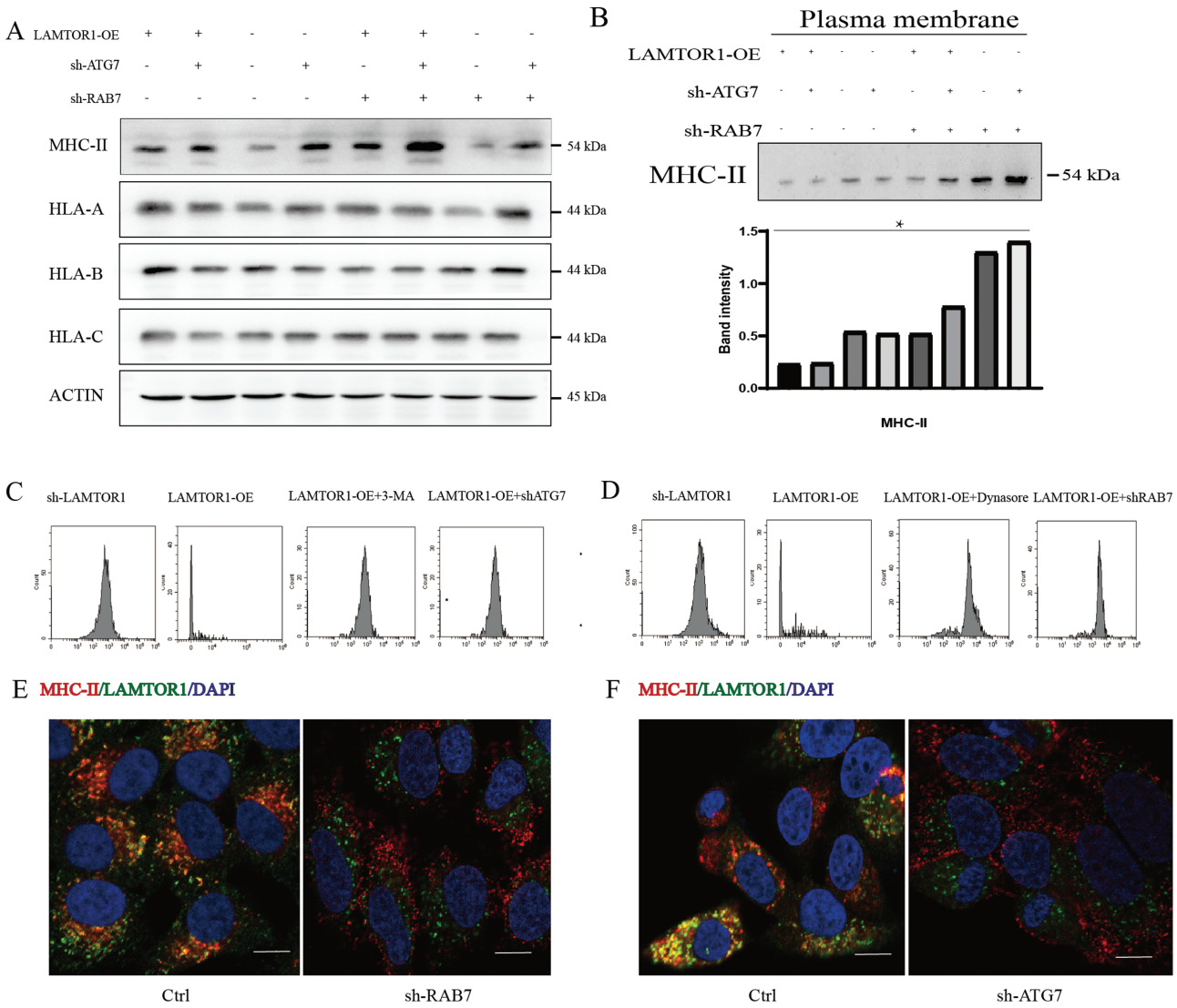

Figure 3. LAMTOR1 promotes MHC-II endocytic trafficking to the lysosome through an autophagy-dependent pathway. (**A**) Treatment of Huh7, HepG2 and Hepa1-6 cells overexpressing *LAMTOR1* with sh-*RAB7* or/and sh-*ATG7* to detect the effect of MHC-II, HLA-A, HLA-B and HLA-C expression levels. (**B**) Effect of sh-*RAB7* as well as sh-*ATG7* on plasma membrane MHC-II was detected by immunoblotting. (**C**) Flow cytometry plot showing plasma membrane MHC-II expression after knockdown of *ATG7* and inhibitor 3-MA. (**D**) Flow cytometry plot showing plasma membrane MHC-II expression after knockdown of *RAB7* and inhibitor Dynasore. (**E, F**) Localization of LAMTOR1 relative to MHC-II (red) in cells treated with sh-*RAB7* and sh-*ATG7*.

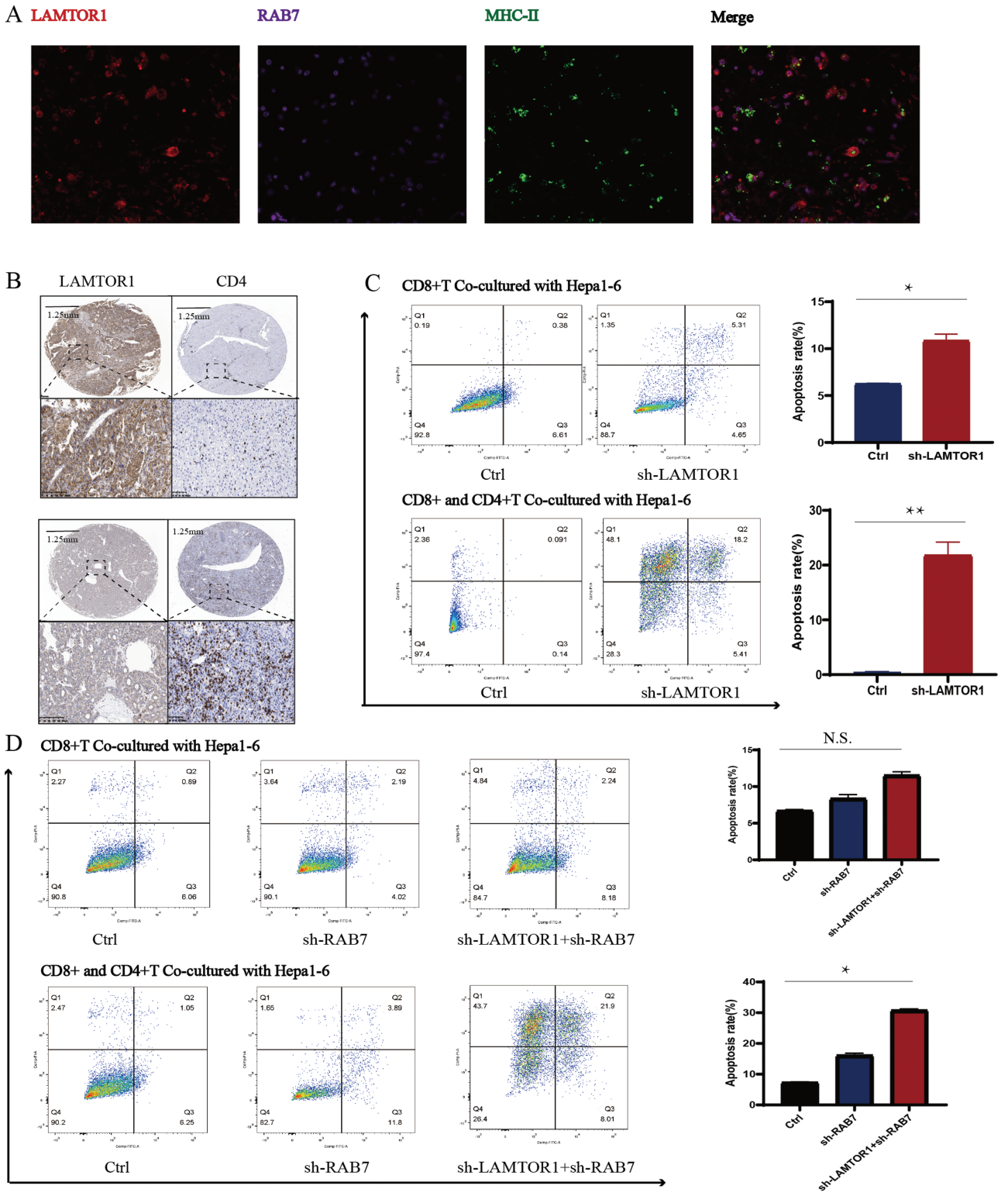

Figure 4. LAMTOR1 trafficking to the endocytic pathway inhibits the antitumor T cell response. (**A**) Colocalization of LAMTOR1, RAB7 and MHC-II in HCC cell. (**B**) IHC staining showing positive correlation of LAMTOR1 expression with CD4 (scale bar: 200 μm; scale bar: 1.25 mm). (**C**) Flow cytometry analysis of cell lines cocultured with $CD4^+$ T, $CD8^+$ T cells to test apoptosis. (**D**) Flow cytometry analysis of cell lines cocultured with $CD4^+$ T, $CD8^+$ T cells to test apoptosis.

of serial sections on tissue microarrays (n = 45) (Figure 4B). To assess antigen presentation, $CD8^+$, and $CD4^+$ T cells were cocultured with mouse Hepa1-6 cells pretreated with *sh-LAMTOR1* and were found to show substantially higher tumor cell apoptosis compared with coculture with $CD8^+$ T cells alone ($P < 0.05$) (Figure 4C). In addition, $CD8^+$ and $CD4^+$ T cells were cocultured with mouse Hepa1-6 cells pretreated with *sh-LAMTOR1+shRAB7* and were found to

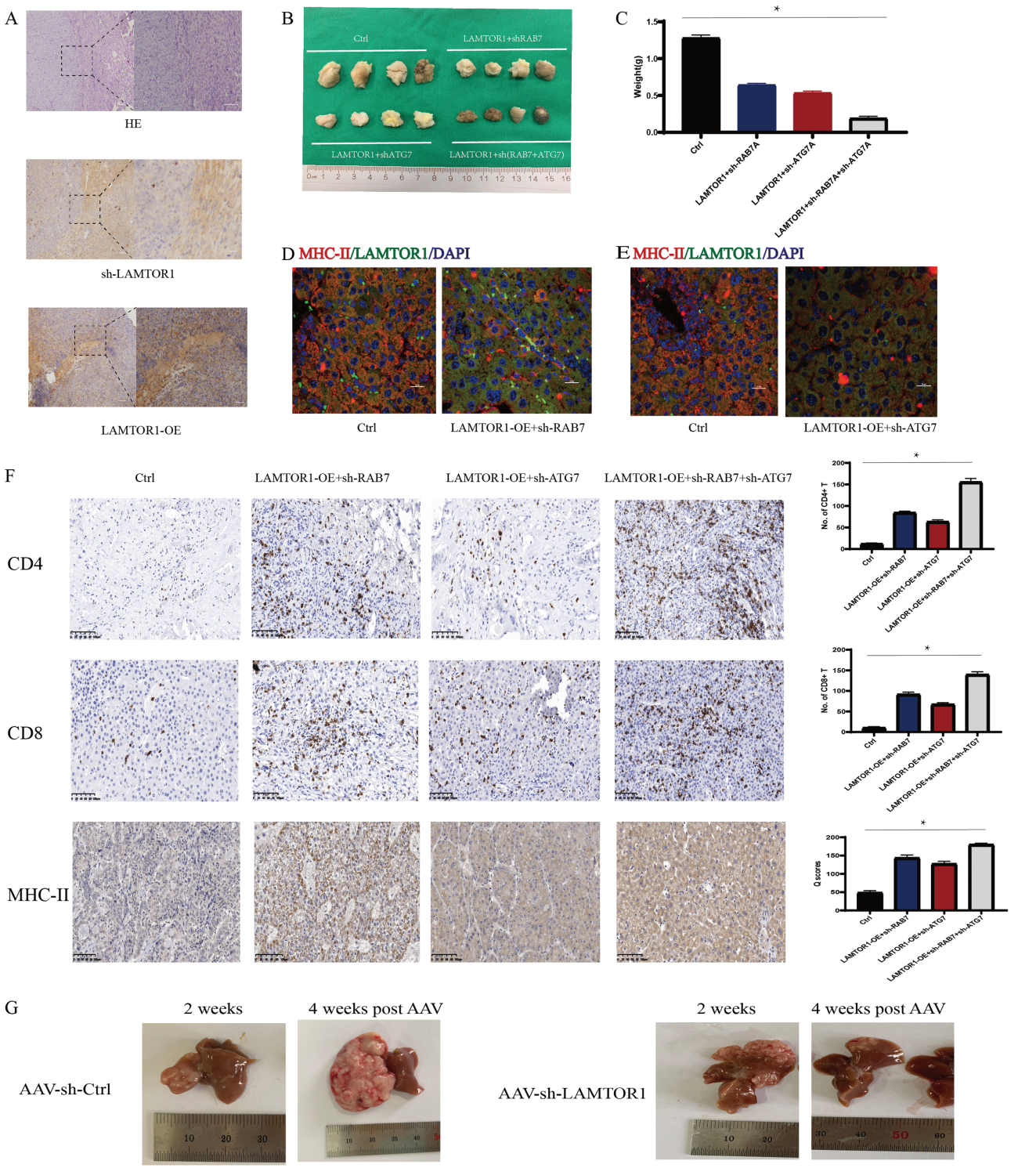

Figure 5. LAMTOR1 promotes tumor development through endocytic pathway *in vivo*. (**A**) Mouse Hepa1-6 cells were transplanted into homozygous (C57BL/6) mice for implantation, and expression analysis was performed using hematoxylin and eosin and IHC for LAMTOR1 staining in mouse liver cancer samples. (**B, C**) Mouse Hepa1-6 cells were transplanted into homozygous (C57BL/6) mice. (**B**) Tumor images at the endpoint. (**C**) Tumor weight. (**D, E**) Immunofluorescence staining images showing the localization of MHC-II and LAMTOR1 within sh-*RAB7*- or sh-*ATG7*-treated homozygous (C57BL/6) mice. Scale bar: 20 μm. (**F**) IHC staining showing positive expression of $CD8^+$ T and $CD4^+$ T (scale bar: 100 μm). (**G**) Representative images of livers of tumor-bearing mice compared with control AAV mice highlighting the tumor attenuating effect of sh-*LAMTOR1*.

show substantially higher tumor cell apoptosis compared with coculture with $CD8^+$ T cells alone ($P < 0.05$) (Figure 4D). These studies suggest that $CD4^+$ T cells play an important role in tumor-specific killing by $CD8^+$ T cells. We further clarified that the surface level of MHC-II degraded via the endocytic pathway may lead to evasion of recognition by $CD4^+$ T cells, which in turn inhibits the production of tumor-killing $CD8^+$ T cells.

LAMTOR1 can switch the cell surface expression of MHC-II and promote tumor development in HCC

To verify the key role of endocytosis in tumor development, we performed tumor studies in mice and found that the change in expression of LAMTOR1 clearly influenced the degree of malignancy after administration for 2 weeks (Figure 5A). Interestingly, combination therapy completely inhibited tumor growth ($P < 0.05$) (Figure 5B and C). Treatment with *LAMTOR1-OE*+shRAB7 or *LAMTOR1-OE*+shATG7 increased the surface levels of MHC-II *in vivo* (Figure 5D and E). We examined the CD4, CD8 and MHC-II expression *in vivo* treatment with *LAMTOR1-OE*+shRAB7, *LAMTOR1-OE*+shATG7 or *LAMTOR1-OE*+shRAB7 +*shATG7*, the results showed that $CD8^+$ T and $CD4^+$ T cells higher infiltration and the expression with MHC-II was associated with *LAMTOR1-OE*+shRAB7+*shATG7* group ($P < 0.05$) (Figure 5F). The total tumor area dramatically decreased in AAV-*LAMTOR1* mice killed four weeks after treatment, thus demonstrating that AAV-*LAMTOR1* persisted as the tumors progressed (Figure 5G). Therefore, these results confirm that LAMTOR1 downregulated the expression of surface levels of MHC-II and reduced tumor cell death.

Discussion

Endocytosis is a key regulator of immunogenicity in HCC. LAMTOR1 expression was related to the stage in HCC. Our results suggest that LAMTOR1 regulates endocytosis by interacting with the GTPase domain of DNM2 and triggers the formation of endosomes and autophagosomes, which induces the production of amphisome bodies. We further clarified that the surface level of MHC-II degraded via the endocytic pathway may lead to evasion of recognition by $CD4^+$ T cells, which in turn inhibits the production of tumor-killing $CD8^+$ T cells. Therefore, these results confirm that LAMTOR1 downregulated the expression of surface levels of MHC-II and reduced tumor cell death. This is consistent with a recent study that states that autophagy targets intracellular and extracellular components of lysosomal degradation, which leads to antigen processing for MHC presentation and affects the transport of MHC-I molecules (37).

$CD8^+$ T cell responses are often considered to represent the most important immune cell type for controlling tumor growth, and it has been observed that tumors can immune escape by downregulating MHC class I expression (2–5,38–40). Tumor-specific $CD4^+$ T cells provide the task of helper signaling, when $CD4^+$ T and $CD8^+$ T lymphocytes are present together, T cell responses and tumor rejection are greatly enhanced, whereas $CD8^+$ T cell transfer alone is not sufficient to induce tumor remission. Consistently, tumor-specific $CD4^+$ T cells help to maintain the function of tumor-directed $CD8^+$ T cells. The presence of tumor-specific $CD4^+$ T cells enhances the recruitment, proliferation and effector functions of $CD8^+$ T cells through IFN-γ and IL-2 production (2–5,38–40). $CD4^+$ T cells can further enhance the function of $CD8^+$ T cells with high-affinity TCRs. Given the critical role of endocytic systems in supporting cancer metabolism and growth, our data elucidate the relevant functions of the endocytic system in the immune escape of HCC.

Endocytic receptor movement is coordinated by ubiquitinated Rab GTPases, SNARE and endosomal subgroups of regulators and effectors (41,42). RAB5, RAB7, RAB35, TSG101, VPS26A and DNM2 have now been identified to play a role in the vesicle trafficking and endocytic pathways. Interestingly, our results suggest that LAMTOR1 promotes endocytosis by regulating RAB7, RAB35 and TSG101. Pharmacologically, the DNM2 inhibitor Dynasore similarly regulates the expression of TSG101 as well as RAB35. DNM2 is a GTPase that directly interacts with caveolin to mediate membrane division and endosome formation (43) and is a key regulator mediating the independent endocytosis of caveolin (44). Importantly, our data demonstrated that LAMTOR1 is a key regulator mediating the non-dependent endocytosis of caveolin proteins.

The endocytic recruitment of microenvironmental substances to lysosomes is regulated by autophagy, a process that helps to expand the concept of autophagy-mediated organelle homeostasis. Selective degradation of the endoplasmic reticulum, mitochondria and ribosomes has been shown to be essential for various cellular processes (45,46). The localization of autophagy-related proteins in endosomes has been observed during amphisome formation (47,48). Targeting late endosomes by autophagy revealed that endosomes and autophagy disrupt the membrane-associated expression and functional role of MHC-II. These phenomena contribute to the understanding of the role of endosomal and autophagic proteins in MHC-II transport. It follows that the balanced role of endosomes and autophagy affects important physiological and pathological processes such as development, immunity and cancer (49). Moreover, in endosome-deficient tumor models, MHC-II is considered a key driver of oncogenic effects and can be an important strategy for tumor survival by avoiding immune recognition and attack. There are some shortcomings in this study, we were not able to verify the validity of the study by CRISPR-edited mice, and we were not able to explore the binding site of LAMTOR1 to DNM2. In this study, we explored the interaction of MHC-II with endocytosis, gathered mechanistic insights into how endocytosis contributes to immune escape and provide a strong rationale for developing novel therapeutic approaches for patients with HCC. Furthermore, anti-LAMTOR1 could support other approaches such as cancer vaccinations in HCC as it increases the immunogenicity by augmenting the antigen presentation in T cells.

Supplementary material

Supplementary data are available at *Carcinogenesis* online.

Supplementary Fig 1. Representative image of IHC staining for LAMTOR1 expression in 45 HCC patients (scale bar:1.25 mm).

Supplementary Fig 2. A, Confocal co-localization analysis of endogenous RAB5 (red) and LAMTOR1 (green) in human HCC and adjacent tissues. Scale bar:20 μm. B, C, Fluorescence microscopy and western blot images of EGFR in sh-Ctrl and sh-LAMTOR1 cells. Scale bar:20 μm. D, Dynasore-treated cells for 0.5, 1, 2, 4 and 6 h to disrupt endocytosis followed by western blotting.

Supplement Fig 3. LAMTOR1 accelerates the fusion of autophagosomes and endosomes. A, The effects of sh-Ctrl and sh-LAMTOR1 pretreated with Earle's balanced salt solution and mammalian target of rapamycin (10 nM) on LC3 and P62 protein levels in Huh7, HepG2, and Hepa1-6 cells were analyzed using western blotting. B, Amount of autophagosomes of Huh7, HepG2, and Hepa1-6 cells with

Ctrl or sh-LAMTOR1. Arrows represent autophagic vacuoles (scale bar:1 μm). C, D, Confocal analysis of endogenous LC3 (red) and TSG101 (green) with HCC tissues or cells treated with sh-Ctrl or sh-LAMTOR1. Scale bar:20 μm. E, F, Confocal analysis of endogenous LC3 (red) and CD63 (green) with HCC tissues or cells treated with sh-Ctrl or sh-LAMTOR1. Scale bar:20 μm. G, H, Confocal analysis of endogenous LAMP1 (green), LC3B (red), and CD63 (green) in HCC tissues or cells treated with sh-Ctrl or sh-LAMTOR1. Scale bar:20 μm.

Supplementary Fig 4. A, Confocal co-localization analysis of endogenous LC3 (red) and LAMP1 (green) in human HCC and adjacent tissues. Scale bar:20 μm. B, Fluorescence microscopy images of endogenous CD63 (red) and LAMP1 (green) in human HCC and adjacent tissues. Scale bar:20 μm.

Supplementary Fig 5. A-D, Endocytic pathway positively correlated with cell adhesion (CAM) and (A) immune cell, (B) extracellular vesicle, (C) and stem cell (D) expression from the TCGA data of HCC. E, Heat map showing 11 differentially expressed genes associated with LAMTOR1 of CAM based on TCGA datasets. F, Data analysis revealed that memory CD4+ T cells were associated with LAMTOR1 based on GSE140228 datasets.

Supplementary Fig 6. LAMTOR1 is involved with cell adhesion molecules (CAM). A, B, The correlation between endocytosis and CAM were validated by univariate and multivariate Cox regression analysis. C, Gene Set Enrichment analysis (GSEA) of LAMTOR1 using the TCGA dataset showing the extent of enrichment of CAM gene features in HCC cells. NES, normalized enrichment score. D, The relationship of enrichment of top 40 CAM gene sets with LAMTOR1 expression level. Signature gene sets were used to run GO analysis. E, F, EdU and cell migration assays demonstrating the effect of sh-LAMTOR1 on cell proliferation and migration (scale bar:10 μm). G, H, Localization of MHC-II (red) relative to CD63 (green) (G) and LC3B (green) (I) in HCC and adjacent tissues. Scale bar:20 μm.

Supplementary Fig. 7A-D, Treatment of Huh7, HepG2, and Hepa1-6 cells overexpressing LAMTOR1 with sh-RAB7 or/and sh-ATG7 to detect the effects of MHC-II, HLA-A, HLA-B, and HLA-C expression levels.

Funding

This work was supported by the National Natural Science Foundation of China (No.81901434, No.81970466), China Postal Science Foundation (No.2018M641743, No.2019M661168) and Natural Science Foundation of Liaoning Province (2019-ZD-0784).

Acknowledgments

Conflict of Interest Statement: This manuscript has been read and approved by all authors and all declare that they have no competing interests.

Author contributions

BW and MX-J contributed to conception and design of the study. BW, QW, and MX-J performed the in vitro experiments with cell lines. BW-L provided expertise in mouse models. BW and BW-L carried out the TCGA data set analysis. BW provided expertise in statistical analysis. BW and QW drafted the manuscript. MX-J revised the manuscript critically for important intellectual content.

Data availability

All experimental data during this research are included in the published article and its supplementary files. The datasets and materials in this study are available on reasonable request from corresponding authors.

References

1. Sung, H. et al. (2021) Global cancer statistics 2020: GLOBOCAN estimates of incidence and mortality worldwide for 36 cancers in 185 countries. *CA. Cancer J. Clin.*, 71, 209–249.
2. Borst, J. et al. (2018) CD4(+) T cell help in cancer immunology and immunotherapy. *Nat. Rev. Immunol.*, 18, 635–647.
3. Alspach, E. et al. (2019) MHC-II neoantigens shape tumour immunity and response to immunotherapy. *Nature*, 574, 696–701.
4. McCaw, T.R. et al. (2019) The expression of MHC class II molecules on murine breast tumors delays T-cell exhaustion, expands the T-cell repertoire, and slows tumor growth. *Cancer Immunol. Immunother.*, 68, 175–188.
5. Quezada, S.A. et al. (2010) Tumor-reactive CD4(+) T cells develop cytotoxic activity and eradicate large established melanoma after transfer into lymphopenic hosts. *J. Exp. Med.*, 207, 637–650.
6. Muller, M. et al. (2015) The coordinated action of the MVB pathway and autophagy ensures cell survival during starvation. *Elife*, 4, e07736.
7. Nassour, J. et al. (2019) Autophagic cell death restricts chromosomal instability during replicative crisis. *Nature*, 565, 659–663.
8. Monypenny, J. et al. (2018) ALIX regulates tumor-mediated immunosuppression by controlling EGFR activity and PD-L1 presentation. *Cell Rep.*, 24, 630–641.
9. Fraser, J. et al. (2019) Targeting of early endosomes by autophagy facilitates EGFR recycling and signalling. *EMBO Rep.*, 20, e47734.
10. Peng, X. et al. (2020) Focus on the morphogenesis, fate and the role in tumor progression of multivesicular bodies. *Cell Commun. Signal.*, 18, 122.
11. Zoncu, R. et al. (2009) A phosphoinositide switch controls the maturation and signaling properties of APPL endosomes. *Cell*, 136, 1110–1121.
12. Grant, B.D. et al. (2009) Pathways and mechanisms of endocytic recycling. *Nat. Rev. Mol. Cell Biol.*, 10, 597–608.
13. Anding, A.L. et al. (2017) Cleaning house: selective autophagy of organelles. *Dev. Cell.*, 41, 10–22.
14. Jia, J. et al. (2018) Galectins Control mTOR in response to endomembrane damage. *Mol. Cell.*, 70, 120–135 e128.
15. Puri, C. et al. (2018) The RAB11A-positive compartment is a primary platform for autophagosome assembly mediated by WIPI2 recognition of PI3P-RAB11A. *Dev. Cell*, 45, 114–131 e118.
16. Soreng, K. et al. (2018) SNX18 regulates ATG9A trafficking from recycling endosomes by recruiting Dynamin-2. *EMBO Rep.*, 19.
17. Fader, C.M. et al. (2009) TI-VAMP/VAMP7 and VAMP3/cellubrevin: two v-SNARE proteins involved in specific steps of the autophagy/multivesicular body pathways. *Biochim. Biophys. Acta.*, 1793, 1901–1916.
18. Jager, S. et al. (2004) Role for Rab7 in maturation of late autophagic vacuoles. *J. Cell Sci.*, 117, 4837–4848.
19. Takahashi, Y. et al. (2018) An autophagy assay reveals the ESCRT-III component CHMP2A as a regulator of phagophore closure. *Nat. Commun.*, 9, 2855.
20. Dai, C. et al. (2001) PDGF autocrine stimulation dedifferentiates cultured astrocytes and induces oligodendrogliomas and oligoastrocytomas from neural progenitors and astrocytes in vivo. *Genes Dev.*, 15, 1913–1925.

21. Nada, S. et al. (2009) The novel lipid raft adaptor p18 controls endosome dynamics by anchoring the MEK-ERK pathway to late endosomes. *EMBO J.*, 28, 477–489.
22. Nowosad, A. et al. (2020) p27 controls Ragulator and mTOR activity in amino acid-deprived cells to regulate the autophagy-lysosomal pathway and coordinate cell cycle and cell growth. *Nat. Cell Biol.*, 22, 1076–1090.
23. Filipek, P.A. et al. (2017) LAMTOR/Ragulator is a negative regulator of Arl8b- and BORC-dependent late endosomal positioning. *J. Cell Biol.*, 216, 4199–4215.
24. Nakase, I. et al. (2015) Active macropinocytosis induction by stimulation of epidermal growth factor receptor and oncogenic Ras expression potentiates cellular uptake efficacy of exosomes. *Sci. Rep.*, 5, 10300.
25. Feng, D. et al. (2010) Cellular internalization of exosomes occurs through phagocytosis. *Traffic*, 11, 675–687.
26. Barres, C. et al. (2010) Galectin-5 is bound onto the surface of rat reticulocyte exosomes and modulates vesicle uptake by macrophages. *Blood*, 115, 696–705.
27. Nanbo, A. et al. (2013) Exosomes derived from Epstein-Barr virus-infected cells are internalized via caveola-dependent endocytosis and promote phenotypic modulation in target cells. *J. Virol.*, 87, 10334–10347.
28. Puri, C. et al. (2020) A DNM2 centronuclear myopathy mutation reveals a link between recycling endosome scission and autophagy. *Dev. Cell*, 53, 154–168.e6.
29. Palusova, V. et al. (2020) Dual targeting of BRAF and mTOR signaling in melanoma cells with pyridinyl imidazole compounds. *Cancers (Basel)*, 12:1516.
30. Omi, J. et al. (2020) The inducible amphisome isolates viral hemagglutinin and defends against influenza A virus infection. *Nat. Commun.*, 11, 162.
31. Wang, K. et al. (2019) Mechanical stress-dependent autophagy component release via extracellular nanovesicles in tumor cells. *ACS Nano.*, 13, 4589–4602.
32. Fader, C.M. et al. (2008) Induction of autophagy promotes fusion of multivesicular bodies with autophagic vacuoles in k562 cells. *Traffic*, 9, 230–250.
33. Nino, C.A. et al. (2019) When ubiquitin meets E-cadherin: plasticity of the epithelial cellular barrier. *Semin. Cell Dev. Biol.*, 93, 136–144.
34. Polo, S. et al. (2006) Endocytosis conducts the cell signaling orchestra. *Cell*, 124, 897–900.
35. Chao, M.P. et al. (2012) The CD47-SIRPalpha pathway in cancer immune evasion and potential therapeutic implications. *Curr. Opin. Immunol.*, 24, 225–232.
36. Kalluri, R. et al. (2020) The biology, function, and biomedical applications of exosomes. *Science*, 367, eaau6977.
37. Munz, C. (2020) Autophagy proteins influence endocytosis for MHC restricted antigen presentation. *Semin. Cancer Biol.*, 66, 110–115.
38. Coulie, P.G. et al. (2014) Tumour antigens recognized by T lymphocytes: at the core of cancer immunotherapy. *Nat. Rev. Cancer.*, 14, 135–146.
39. Hulpke, S. et al. (2013) The MHC I loading complex: a multitasking machinery in adaptive immunity. *Trends Biochem. Sci.*, 38, 412–420.
40. Nagasaki, J. et al. (2020) The critical role of CD4+ T cells in PD-1 blockade against MHC-II-expressing tumors such as classic Hodgkin lymphoma. *Blood Adv.*, 4, 4069–4082.
41. Pfeffer, S.R. (2013) Rab GTPase regulation of membrane identity. *Curr. Opin. Cell Biol.*, 25, 414–419.
42. Zhen, Y. et al. (2015) Cellular functions of Rab GTPases at a glance. *J. Cell Sci.*, 128, 3171–3176.
43. Yao, Q. et al. (2005) Caveolin-1 interacts directly with dynamin-2. *J. Mol. Biol.*, 348, 491–501.
44. Mayor, S. et al. (2014) Clathrin-independent pathways of endocytosis. *Cold Spring Harb. Perspect. Biol.*, 6, a016758.
45. Gatica, D. et al. (2018) Cargo recognition and degradation by selective autophagy. *Nat. Cell Biol.*, 20, 233–242.
46. Rogov, V. et al. (2014) Interactions between autophagy receptors and ubiquitin-like proteins form the molecular basis for selective autophagy. *Mol Cell*, 53, 167–178.
47. Florey, O. et al. (2011) Autophagy machinery mediates macroendocytic processing and entotic cell death by targeting single membranes. *Nat. Cell Biol.*, 13, 1335–1343.
48. Hoyvik, H. et al. (1991) Inhibition of autophagic-lysosomal delivery and autophagic lactolysis by asparagine. *J. Cell Biol.*, 113, 1305–1312.
49. He, X. et al. (2020) Immune checkpoint signaling and cancer immunotherapy. *Cell Res.*, 30, 660–669.